Control of single-stage single-phase PV inverter

Mihai Ciobotaru, Remus Teodorescu and Frede Blaabjerg
Institute of Energy Technology
Aalborg University
Pontoppidanstraede 101
DK-9220, Aalborg, Denmark
Tel.: +45 / 9635 9252
Fax: +45 / 2539 4182
E-Mail: mpc@iet.aau.com, ret@iet.aau.com, fbl@iet.aau.com
URL: http://www.iet.aau.dk

Keywords

«Distributed power», «Harmonics», «Photovoltaic», «Single phase system», «Solar Cell System»

Abstract

In this paper the issue of control strategies for single-stage photovoltaic (PV) inverter is addressed. Two different current controllers have been implemented and an experimental comparison between them has been made. A complete control structure for the single-phase PV system is also presented. The main elements of the PV control structure are: - a maximum power point tracker (MPPT) algorithm using the incremental conductance method; - a synchronization method using the phase-locked-loop (PLL), based on delay; - the input power control using the dc voltage controller and power feed-forward; - and the grid current controller implemented in two different ways, using the classical proportional integral (PI) and the novel proportional resonant (PR) controllers. The control strategy was tested experimentally on 1.5 kW PV inverter.

Introduction

The market for PV power applications continues to develop at a high rate. Between 2002 and 2003 the total installed capacity in the International Energy Agency (IEA) Photovoltaic Power Systems (PVPS) countries grew by 36 %, reaching 1 809 MW. Moreover, the price level of the PV modules and the system costs (inverter included) has decreased significantly. The use to PV systems connected in parallel with the mains was simplified and is often supported by incentives from utilities and/or governmental bodies. Before connecting a PV system to the power network, the dc voltage of the solar modules must be converted into an ac voltage. Some protection systems are required to prevent damage in the PV system caused by the utility network and vice versa. The PV systems require standards addressing the use and the performance of grid-connected PV inverters, thus ensuring the safety and quality of the manufacture.

The purpose of the power electronics in PVPS is to convert the dc current from the PV panels into ac current to the grid, with the highest possible efficiency, the lowest cost and to keep a superior performance. The basic interfacing is shown in Fig. 1.

A controversial issue for PV inverters is the harmonics level. The IEEE 929 standard permits a limit of 5% for the current total harmonic distortion (THD) factor with individual limits of 4% for each odd harmonic from 3^{rd} to 9^{th} and 2% for 11^{th} to 15^{th} while a recent draft of European IEC61727 suggests almost the same thing as previously mentioned. These levels are far more stringent than other domestic appliances, like

IE61000-3-2, as PV systems are viewed as generation sources and so are subject to higher standards than load systems.

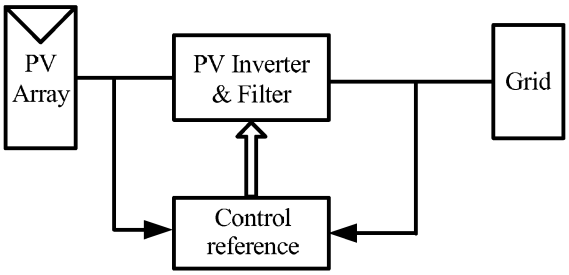

Fig. 1: Power electronic system with the grid, source (PV array), power converter and control

For current-controlled PV inverters in most of the cases we make use of PI controller with grid voltage feed-forward (VFF) [1], [2], but this solution exhibits two well known drawbacks (due to the poor performance of the integral action): inability of the PI controller to track a sinusoidal reference without steady-state error and poor disturbance rejection capability. An alternative solution in order to alleviate the PI's drawbacks is presented in [3], where a second order generalized integrator (GI) can be used. The GI is a double integrator that achieves an "infinite" gain at a certain frequency (resonance frequency), and almost no attenuation exists outside this frequency. Thus, it can be used as a notch filter in order to compensate the harmonics in a very selective way. Another approach reported in [4] where a new type of stationary-frame regulators called Proportional Resonant (PR) is introduced. In this approach the classical PI dc-compensator is transformed into an equivalent ac-compensator having the same frequency response characteristics in the bandwidth of concern.

This paper is aimed at presenting a single-stage converter for single-phase PV systems. Two different current controllers have been implemented and an experimental comparison between them has been made. A complete control structure for the single-phase PV system is also presented. An incremental conductance method has been used in order to track the MPPT of the PV characteristic. In order to get a clean sinusoidal current reference (synchronized with the grid voltage) it is used a PLL, a based on delay structure. The conclusions are presented in the final part of the paper.

System description

Usually the power converter interface from the dc source to the load and/or to the grid consists of a two-stage converter: the dc-dc converter and the dc-ac converter. An interesting alternative solution could be the use of a single-stage converter where the dc-dc converter is avoided and in order to ensure the necessary dc voltage level the PV array can be a string of PV panels or a multitude of parallel strings of PV panels. In the classical solution with two-stage converter, the dc-dc converter requires several additional devices producing a large amount of conduction losses, sluggish transient response and high cost while the advantages of the single-stage converters are: good efficiency, a lower price and easier implementation. The disadvantages of the single-stage converter are the fact that the PV panels are in series and if the shading occurs on one or several PV panels then the efficiency of the whole system is reduced.

As shown in Fig. 2, the PV inverter system consists of a solar panel string and a dc link capacitor C_{dc} on the dc side with an output ac filter (LCL), insulation transformer and grid connection on the ac side. The number of panels in the string has to ensure a dc voltage higher then the ac voltage peak at all time. The energy conversion from dc to ac side is made by a single-phase voltage source inverter. The used solar-panel string consists of sixteen uniserial PV panels (120 W for each panel).

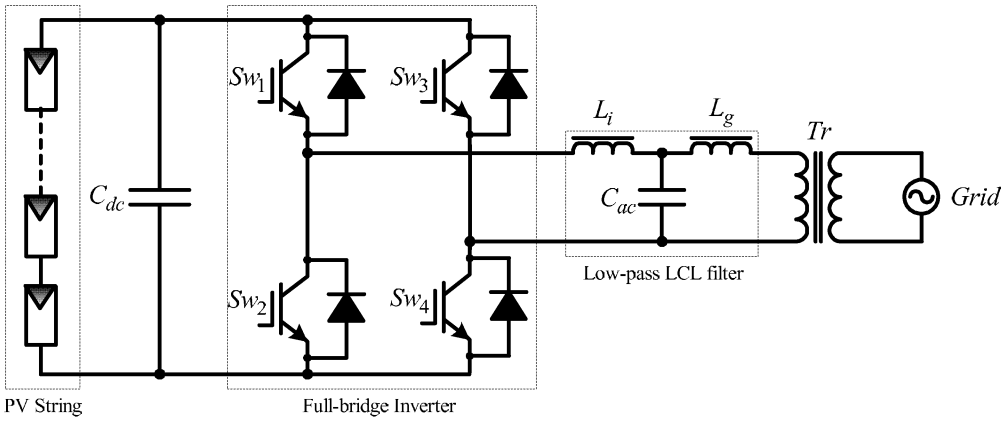

Fig. 2: The voltage source PV inverter connected to the grid through an LCL filter

Control strategy

For the grid-connected PV inverters in the power range of 1-5 kW, the most common control structure for the dc-ac grid converter is a current-controlled H-bridge PWM inverter having a low-pass output filter. Typically L filters are used but the new trend is to use LCL filters that have a higher order (3rd) which leads to more compact design. The drawback is its resonance frequency which can produce stability problems and special control design is required [5]. The control structure of the PV energy conversion system is shown in Fig. 3.

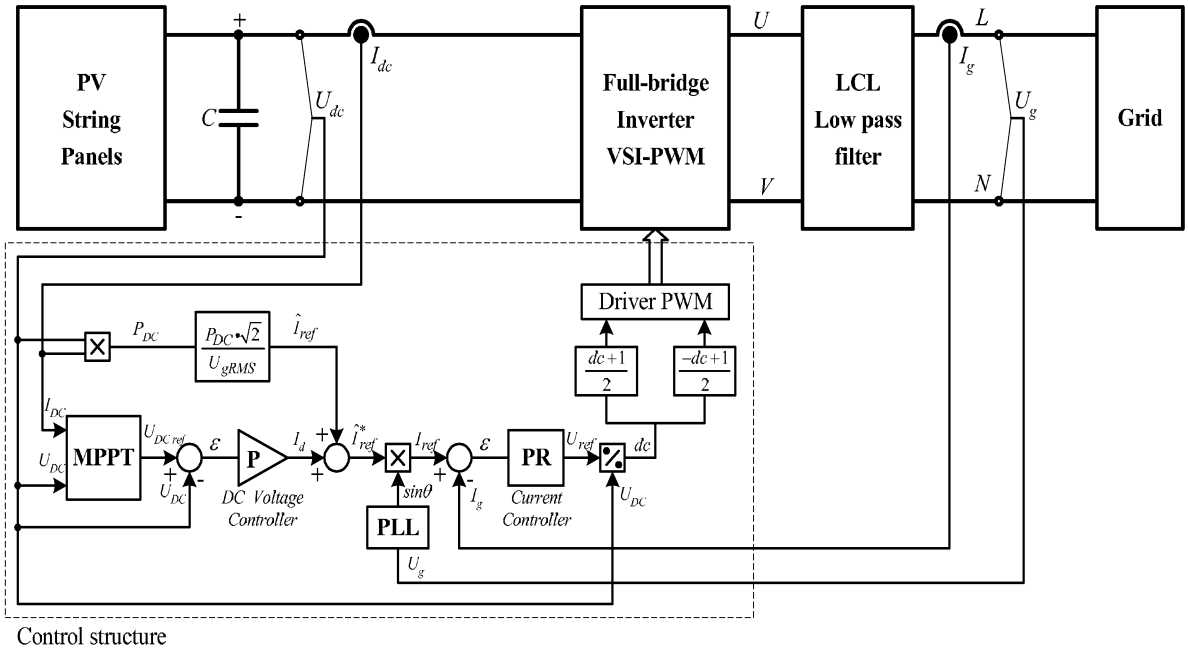

Fig. 3: Control diagram of the PV energy conversion system

The main elements of the control structure are the synchronization algorithm based on PLL, the MPPT, the input power control and the grid current controller.

PLL structure

The PLL is used to provide a unity power factor operation which involves synchronization of the inverter output current with the grid voltage and to give a clean sinusoidal current reference. The PI controller parameters of the PLL structure are calculated in such a way that we can set directly the settling time and the damping factor of this PLL structure. The PLL structure is also used for grid voltage monitoring in order to get the amplitude and the frequency values of the grid voltage. The general form of the PLL structure is presented in Fig. 4.

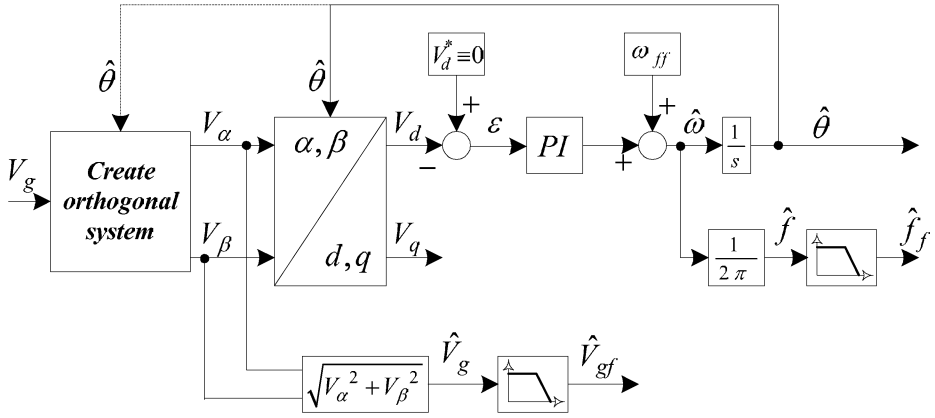

Fig. 4: General structure of a single phase PLL

MPPT algorithm

The task of the MPPT in a PV energy conversion system is to tune continuously the system so that it draws maximum power from the solar array regardless of weather or load conditions. Since the solar array has non ideal voltage-current characteristics and the conditions such as irradiance, ambient temperature, and wind that affect the output of the solar array are unpredictable, the tracker should deal with a nonlinear and time-varying system. The conventional MPPT algorithms are using $dP/dV = 0$ to obtain the maximum power point output. Several algorithms can be used in order to implement the MPPT as follows [6]: perturb and observe, incremental conductance, parasitic capacitance and constant voltage, but only the first two are the most frequently used.

The incremental conductance algorithm has been chosen as a MPPT strategy in this paper. This algorithm has advantages compared to perturb and observe as it can determine when the MPPT has reached the MPP, where perturb and observe oscillates around the MPP. Also, incremental conductance can track rapidly the increase and decrease of irradiance conditions with higher accuracy than perturb and observe.

One disadvantage of this algorithm is the increased complexity when compared to perturb and observe. This increases the computational time and slows down the sampling frequency of the array voltage and current. The flowchart of the incremental conductance algorithm is shown in Fig. 5 [7] where the V_k and I_k are the momentary voltage and current of the PV array and V_{k-1} and I_{k-1} are the previous voltage and current, respectively. The dP/dV term can be replaced by $I + (\Delta I / \Delta V) \cdot V$. The output of the MPPT is the dc voltage reference (V^*_{pv}).

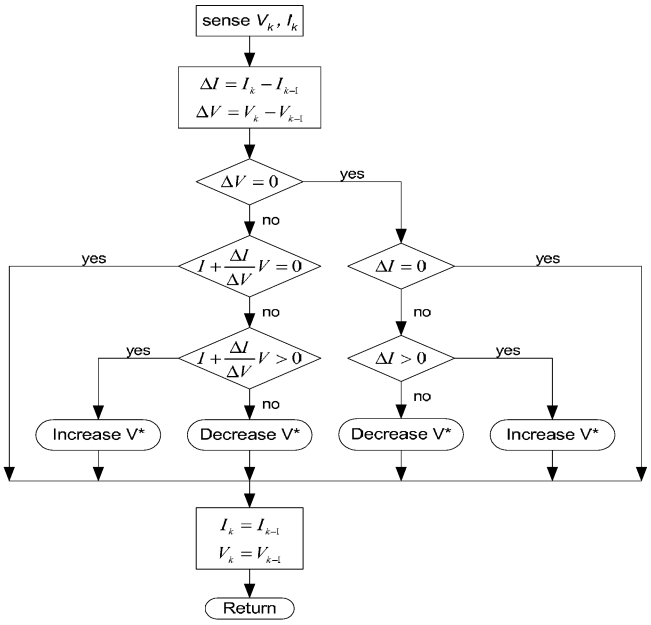

Fig. 5: Flowchart of the incremental conductance algorithm

Input power control

The control strategies of input power in the case of a power configuration of PV system without dc-dc converter are presented in the following section. In Fig. 6 a new control strategy of input power is proposed. The new element introduced is the power feed-forward. The computed value of the current amplitude reference using the PV power (P_{PV}) and the RMS value of the ac voltage ($V_{ac\,RMS}$) is added to the output value of the dc voltage controller ($\hat{I}_r$) resulting in the ac current amplitude reference ($\hat{I}_{ref}$).

Using the input power feed-forward the dynamic of the PV system is improved being known the fact that the MPPT is rather slow. The dc voltage controller ensures a quick response of the PV system at a sudden change of the input power.

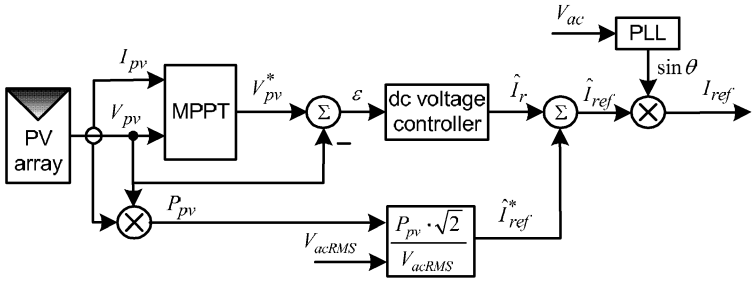

Fig. 6: New control structure of controlling the input power. A feed-forward of input power is used

Grid current controller

Classical PI control with grid voltage feed-forward (U_g) as depicted in Fig. 7a, is commonly used for current-controlled PV inverters.

a) b)

Fig. 7: The current loop of PV inverter: a) with PI controller; b) with PR controller

The PI current controller $G_{PI}(s)$ is defined as:

$$G_{PI}(s) = K_P + \frac{K_I}{s} \tag{1}$$

In order to get a good dynamic response, a grid voltage feed-forward is used, as depicted in Fig. 7a. This leads in turn to stability problems related to the delay introduced in the system by the voltage feedback filter (U_g). In order to alleviate this problem an advanced filtering method for the grid voltage feed-forward should be considered. A Bode diagram analysis of the PI controller is presented in Fig. 8.

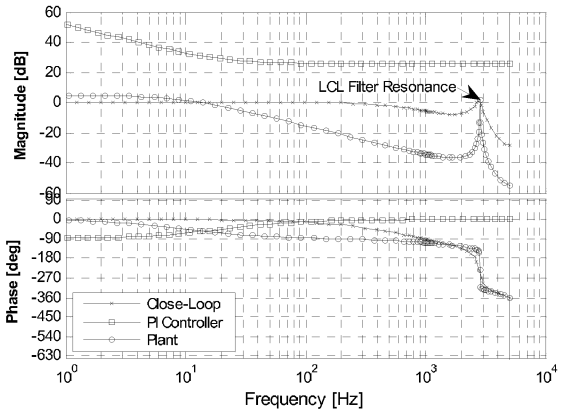

Fig. 8: PI current controller – Bode diagram analysis

As it has been mentioned in the introduction of this paper, an alternative solution for the poor performances of the PI controller is the PR controller. The current loop of the PV inverter with PR controller is shown in Fig. 7b.

The PR current controller $G_c(s)$ is defined as [3], [5]:

$$G_c(s) = K_P + K_I \frac{s}{s^2 + \omega_o^2} \tag{2}$$

The harmonic compensator (HC) $G_h(s)$ as defined in [5]:

$$G_h(s) = \sum_{h=3,5,7} K_{Ih} \frac{s}{s^2 + (\omega_o h)^2} \tag{3}$$

is designed to compensate the selected harmonics 3rd, 5th and 7th as they are the most predominant harmonics in the current spectrum.

A processing delay, usually equal to T_s for the PWM inverters [2], is introduced in $G_d(s)$. The filter transfer function $G_f(s)$ is expressed in (4) [8].

$$G_f(s) = \frac{i_i(s)}{u_i(s)} = \frac{1}{L_i s} \frac{\left(s^2 + z_{LC}^2\right)}{\left(s^2 + \omega_{res}^2\right)} \tag{4}$$

- where $z_{LC}^2 = \left[L_g C_f\right]^{-1}$ and $\omega_{res}^2 = \frac{\left(L_i + L_g\right) \cdot z_{LC}^2}{L_i}$

The current error - disturbance ratio rejection capability at null reference is defined as:

$$\left.\frac{\varepsilon(s)}{u_g(s)}\right|_{i_i^* = 0} = \frac{G_f(s)}{1 + \left(G_c(s) + G_c(s)\right) \cdot G_d(s) \cdot G_f(s)} \tag{5}$$

where: ε is current error and the grid voltage u_g is considered as the disturbance for the system.

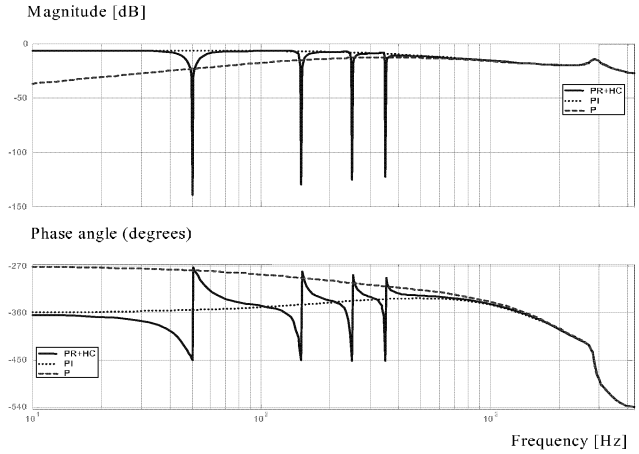

Fig. 9: Bode diagram of the disturbance rejection (current error ratio disturbance) of the PR+HC (3rd, 5th and 7th), PI and P current controllers

In Fig. 9 is presented the Bode diagram of the disturbance rejection for the P, PI and PR controllers. It can be very easily noticed that the PI rejection capability is worse in comparison with the PR and from Fig. 9 it can be observed that the PI rejection capability at 5th and 7th harmonics is comparable with that one of a simple proportion controller, the integral action being irrelevant. Thus, it is demonstrated the superiority of the PR controller respect to the PI in terms of harmonic current rejection.

The close-loop frequency response of the system and also the Bode plots of the PR + HC and the plant are presented in Fig. 10a The Fig. 10b presets the root-locus of the close-loop current control system and the open-loop frequency response of the system.

The size of the proportional gain K_p from PR controller determines the bandwidth and stability phase margin [3], in the same way as for the PI controller. As it can be observed from the open-loop Bode diagram (Fig. 10b) the phase margin (PM) is determined to be equal with 42 deg, indicating a good stability of the system. Also, the dominant poles of the controller are well damped as it can be seen in Fig. 10b exhibiting a damping factor equal with 0.7.

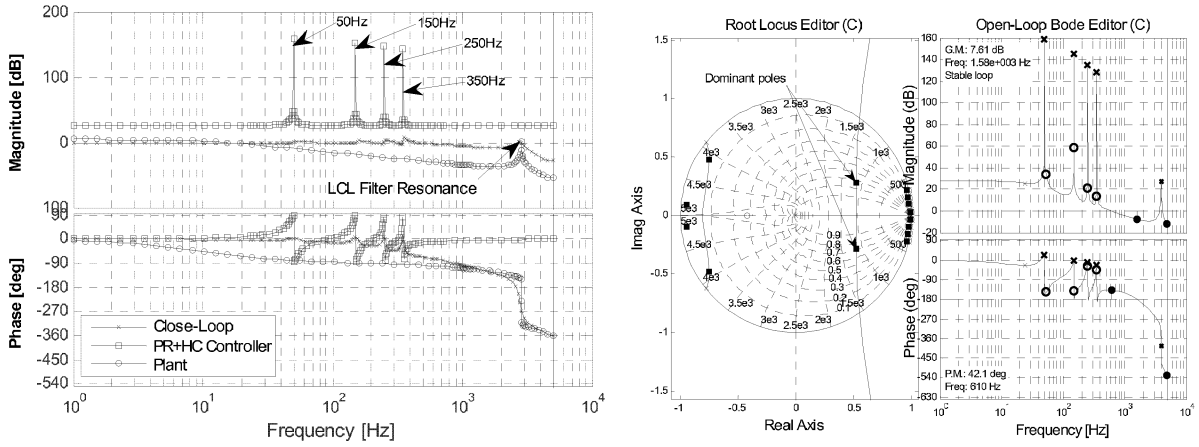

a) b)

Fig. 10: PR current controller – Bode diagrams a) and root-locus b) analysis

Experimental results

A single-stage grid-connected PV inverter (1.5 kW power range) was built in order to analyze the PV systems performance, as depicted in Fig. 11a. The system is dSPACE based and voltage source inverter (VSI) is controlled using a unipolar PWM to place the harmonics on the high frequency side making them easier to filter. The parameters of the LCL filter were: L_i=1426 μH, C_{ac}=2.2 μF, L_g=713 μH. The power stage of a Danfoss VLT 5004 rated 400V/10A was used. The switching frequency of the inverter was 10 kHz. The control algorithm shown in Fig. 3 was implemented using dSPACE DS1103 platform.

The system was tested in the following condition: - the open circuit dc voltage provided by the uniserial sixteen PV panels was around 660 V, the RMS value of the grid voltage was U_g = 225 V with a THD of 2.2 % background distortion. The grid impedance was measured to 1.2 ohms with a series inductance of 2.1 mH because of a insulation transformer using in order to connect the PV system to the grid.

The plotted results have been captured using the graphical interface of the dSPACE system (Control Desk) and then exported to Matlab workspace for plotting.

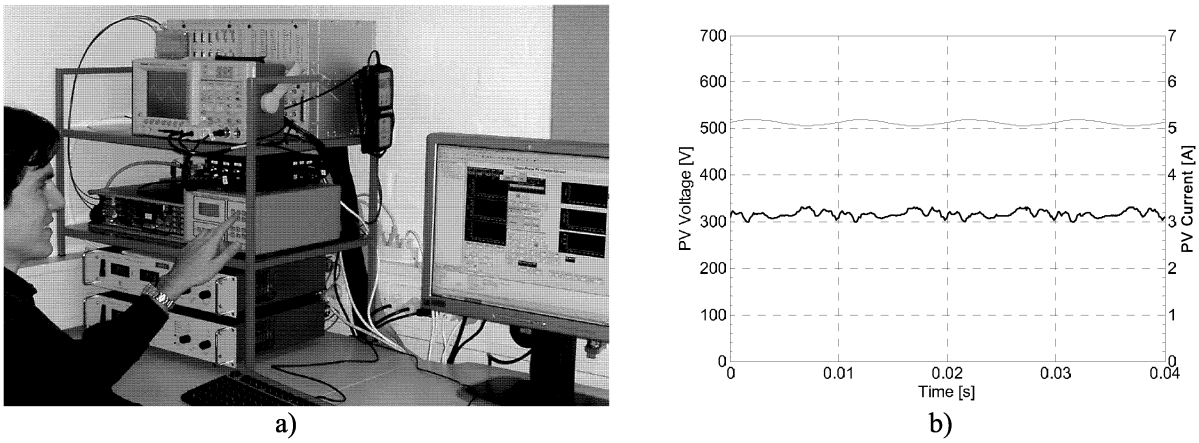

a) b)

Fig. 11: a) Experimental test setup of the 1.5 kW PV inverter; b) PV voltage and current (marked) at 1.5 kW injected power to the grid

The voltage and current of the PV panels at 1.5 kW power on the ac side, are presented in the Fig. 11b.

The grid current and grid voltage at 1.5 kW for PI, PR and PR+HC controllers are presented in Fig. 12 a), b) and c). As it can be seen a much lower THD is obtained with the PR+HC controller. The grid current response at a 5 A step in the current reference is presented for the PI (Fig. 12d), PR (Fig. 12e) and PR+HC (Fig. 12f). As it can be observed the PR and PR+HC controller yields a smaller overshoot than the PI controller.

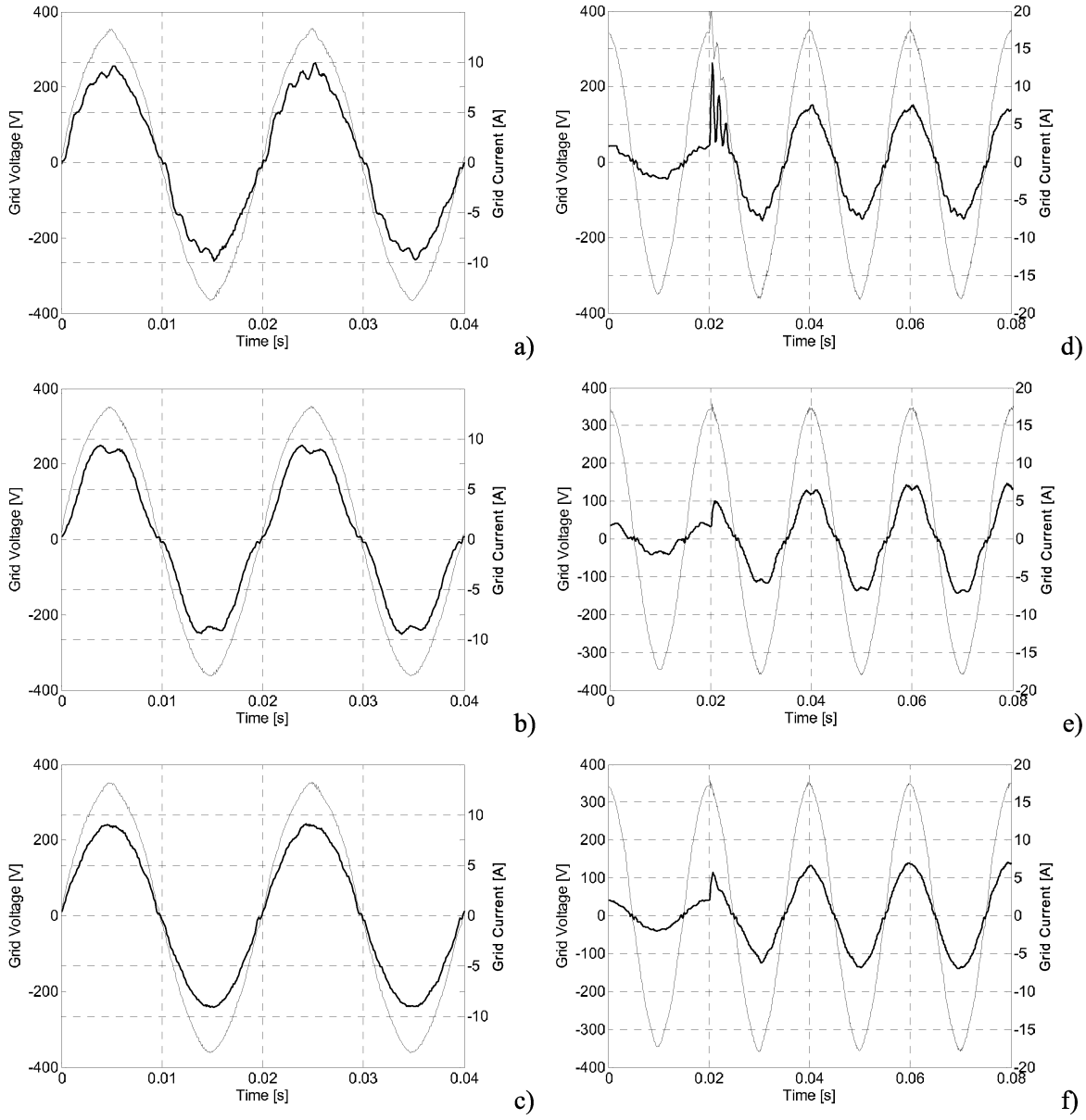

Fig. 12: Grid current (marked) and grid voltage at 1.5 kW for PI a), PR b) and PR+HC c) controllers. Grid current response (marked) at a 5 A step in the current reference for PI d), PR e) and PR+HC f) controllers

In Fig. 13, a comparison of the spectrum for PI, PR and PR+HC in the lower frequency region is presented.

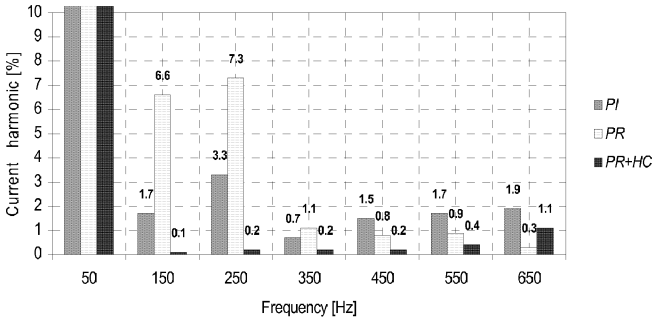

Fig. 13: Measured grid current harmonic spectrum for PI, PR and PR+HC controllers

Using PI controller with VFF has been obtained a current THD of 5.8% while in case of the PR controller the measured current THD was 9.7%. Adding the HC for the PR controller a drastic attenuation of the current THD can be observed, decreasing to 0.5%.

Conclusion

An interesting alternative solution using a single-stage converter, where the dc-dc converter is avoided, has been developed and successfully tested on a dSPACE controlled 1.5kW single-phase PV inverter. The advantages of the single-stage converters are: good efficiency, a lower price and easier implementation, while the main disadvantage is the fact that the PV panels are in series and if the shading occurs on one or several PV panels then the efficiency of the whole system is reduced.

It has been demonstrated that the PR+HC controller gives better performances then the classical PI controller for the grid current loop. The two well known drawbacks of the PI controller are: - steady-state error; and - poor harmonics rejection capability. The steady-state error can be overcame by the PR controller. The PR controller is able to remove the steady-state error without using VFF, which makes it more reliable. By adding the selective HC to the PR controller, a very good rejection for the dominant harmonics can be obtained.

References

[1]. M. Kazmierkovski, R. Krishnan, F. Blaabjerg. Control in Power Electronics, Selected Problems, Academic Press 2002, ISBN 0-12-402772-5.
[2]. C. Cecati, A. Dell'Aquila, M. Liserre and V. G. Monopoli. Design of H-bridge multilevel active rectifier for traction systems, IEEE Trans. on Ind. App., Vol. 39, Sept./Oct. 2003, pp. 1541-1550.
[3]. X. Yuan, W. Merk, H. Stemmler, J. Allmeling. Stationary-Frame Generalized Integrators for Current Control of Active Power Filters with Zero Steady-State Error for Current Harmonics of Concern Under Unbalanced and Distorted Operating Conditions, IEEE Trans. on Ind. App., Vol. 38, No. 2, Mar./Apr. 2002, pp. 523 – 532.
[4]. D. N. Zmood and D. G. Holmes. Stationary Frame Current Regulation of PWM Inverters with Zero Steady-State Error, IEEE Trans. on Power Electronics, Vol. 18, No. 3, May 2003, pp. 814 – 822.
[5]. R. Teodorescu, F. Blaabjerg, M. Liserre, U. Borup. A New Control Structure for Grid-Connected PV Inverters with Zero Steady-State Error and Selective Harmonic Compensation, Proc. of APEC'04, Vol. 1, pp. 580-586.
[6]. D.P. Hohm and M.E. Ropp. Comparative Study of Maximum Power Point Tracking Algorithms Using an Experimental, Programmable, Maximum Power Point Tracking Test Bed, Proc. of Photovoltaic Specialists Conference, 2000, pp.1699 – 1702.
[7]. Y.C. Kuo and T.J. Liang. Novel Maximum-Power-Point-Tracking Controller For Photovoltaic Energy Conversion System, IEEE Transactions on Industrial Electronics, Vol. 48, No. 3 , 2001 pp. 594 – 601.
[8] M. Liserre, F. Blaabjerg and S. Hansen. Design and Control of an LCL-filter Based Active Rectifier, Proc. of IAS'01, Vol. 1, pp. 299-307.